Available online at www.sciencedirect.com
ScienceDirect
Journal of Solid State Chemistry 181 (2008) 751–757
JOURNAL OF SOLID STATE CHEMISTRY
www.elsevier.com/locate/jssc

Preparation and photoluminescence properties of Mn^{2+}-activated $M_2Si_5N_8$ (M = Ca, Sr, Ba) phosphors

C.J. Duan, W.M. Otten, A.C.A. Delsing, H.T. Hintzen*

Materials and Devices for Sustainable Energy Technologies, Department of Chemical Engineering and Chemistry, Eindhoven University of Technology, P.O. Box 513, 5600 MB Eindhoven, the Netherlands

Received 7 August 2007; received in revised form 21 December 2007; accepted 30 December 2007
Available online 6 January 2008

Abstract

Mn^{2+}-doped $M_2Si_5N_8$ (M = Ca, Sr, Ba) phosphors have been prepared by a solid-state reaction method at high temperature and their photoluminescence properties were investigated. The Mn^{2+}-activated $M_2Si_5N_8$ phosphors exhibit narrow emission bands in the wavelength range of 500–700 nm with peak center at about 599, 606 and 567 nm for M = Ca, Sr, Ba, respectively, due to the $^4T_1(^4G) \rightarrow {}^6A_1(^6S)$ transition of Mn^{2+}. The long-wavelength emission of Mn^{2+} ion in the host of $M_2Si_5N_8$ is attributed to the effect of a strong crystal-field of Mn^{2+} in the nitrogen coordination environment. Also it is observed that there exists energy transfer between $M_2Si_5N_8$ host lattice and activator (Mn^{2+}). The potential applications of these phosphors have been pointed out.

Keywords: Luminescence; Phosphor; Nitride material; Manganese

1. Introduction

Recently, the compounds $M_2Si_5N_8$ (M = Ca, Sr, Ba) have been intensively studied as host lattice in exploration of lighting-emitting diode (LED) conversion phosphors [1–9]. Due to the high covalency and large crystal field effect of nitrogen anion, Ce^{3+} and Eu^{2+} show long-wavelength emission in $M_2Si_5N_8$ host lattice (M = Ca, Sr, Ba). These rare-earth doped materials have already been demonstrated to be promising conversion phosphors for white-light LED application [1–9]. Luminescence due to Mn^{2+} is known to occur in a lot of inorganic compounds. Of these, several Mn^{2+}-doped materials are being used widely as fluorescent lamps phosphors, e.g. Zn_2SiO_4:Mn^{2+} (Green) [10] and $BaAl_{12}O_{19}$:Mn^{2+} (Green) [11], and cathode-ray tubes (CRTs) phosphors, e.g. ZnS:Mn^{2+} (Orange) [12,13], $Zn_3(PO_4)_2$:Mn^{2+} (Red) [14,15] and Zn_2SiO_4:Mn^{2+} (Green) [10]. As for the application of Mn^{2+}-doped phosphors in the field of white-light LED, many investigations have been done. However, most of these investigations have focused on Eu^{2+}- and Mn^{2+}-coactivated materials, such as $Ba_3MgSi_2O_8$:Eu^{2+}, Mn^{2+} [16], $CaAl_2Si_2O_8$:Eu^{2+}, Mn^{2+} [17], $SrZn_2(PO_4)_2$:Eu^{2+}, Mn^{2+} [18], $La_{0.827}Al_{11.9}O_{19.09}$:$Eu^{2+}$, Mn^{2+} [19] and so on. In these Eu^{2+}- and Mn^{2+}-coactivated materials, due to the strong absorption of Eu^{2+} in the wavelength range of 250–400 nm and efficient energy transfer from Eu^{2+} to Mn^{2+}, strong green, yellow and /or red emission of Mn^{2+} was obtained besides the blue emission of Eu^{2+} in these materials. Thus, by the color mixing the white light was generated [16–19]. Recently, a new kind of Mn^{2+}-doped LED conversion phosphor has been discovered, namely Ba_2ZnS_3:Mn^{2+} [20–22]. This phosphor shows a broad emission band with peak center at about 625 nm under host excitation of 358 nm. In combination with some other phosphors, white light was also generated [22]. The Mn^{2+} ion usually gives a narrow band emission. The wavelength position of the emission bands depends strongly on the host lattice. It can vary from green to deep red. Mn^{2+} usually gives a green emission when it is located on a lattice site with weak crystal-field, whereas it gives an orange to deep red emission on a strong crystal-field [23]. As far as we know, no reports have been given with regard to the

*Corresponding author. Fax: +31 40 2445619.
E-mail address: h.t.hintzen@tue.nl (H.T. Hintzen).

0022-4596/$ - see front matter © 2008 Elsevier Inc. All rights reserved.
doi:10.1016/j.jssc.2007.12.031

luminescence properties of Mn^{2+} in nitride host lattices except for two publications on the luminescence properties of Mn^{2+} in $MSiN_2$ (M = Mg, Zn, Ca) host lattice [24,25]. In the present work, we focus on studying the luminescence properties of Mn^{2+}-doped $M_2Si_5N_8$ (M = Ca, Sr, Ba) and explore their potential possibilities to be used as new kinds of LED phosphors. This paper is the first one dealing with a systematic study of Mn^{2+} in nitride phosphors of potential interest for white-light LED application.

2. Experimental

2.1. Starting materials

The binary nitride precursors SrN_x ($x \approx 0.6$–0.66) and BaN_x ($x \approx 0.6$–0.66) were prepared by the reaction of the pure strontium metal (Aldrich, 99.9%, pieces) and barium metal (Aldrich, 99.9%, pieces) under flowing dried nitrogen at 800 and 550 °C, respectively, for 8–16 h in a horizontal tube furnace. In addition, Ca_3N_2 powder (Alfa, 98%), α-Si_3N_4 powder (Permascand, P95H, α content 93.2%; Oxygen content: ~1.5%) and Mn powder (Alfa, >99%) are used as the as-received raw materials.

2.2. Syntheses of undoped and Mn^{2+}-doped $M_2Si_5N_8$ (M=Ca, Sr, Ba) samples

Undoped and Mn^{2+}-doped $M_2Si_5N_8$ (M = Ca, Sr, Ba) powder samples were prepared by a solid-state reaction method at high temperature. The appropriate amounts of Ca_3N_2, SrN_x, BaN_x and Mn as well as α-Si_3N_4 powders were weighed out, subsequently mixed and ground together in an agate mortar. The powder mixtures were then transferred into molybdenum crucibles. All processes were carried out in a purified-nitrogen-filled glove-box. Subsequently those powder mixtures were fired twice (with a intermediate grinding in between) in a horizontal tube furnace at 1400 °C for 20 and 24 h, respectively, under flowing 90% N_2–10% H_2 atmosphere. After firing, these samples were gradually cooled down to room temperature in the furnace. There was no apparent reaction of the prepared nitrides with the Mo crucibles. The Mn concentration was taken 5 mol% with respective to the M ions (i.e. $M_{0.95}Mn_{0.05}Si_5N_8$).

2.3. X-ray diffraction data collection and analysis

All measurements were performed on finely ground samples, which were analyzed by X-ray powder diffraction (Rigaku, D/MAX-B) using Cu$K\alpha$ radiation at 40 kV and 30 mA with a graphite monochromator. The phase formation is checked by the normal scan (0.6°/min) in the range of 10–90° 2θ. The XRD measurements were performed at room temperature in air. All the samples are shown to be single phase and the X-ray diffraction patterns of undoped or Mn^{2+}-doped $Ca_2Si_5N_8$, $Sr_2Si_5N_8$ and $Ba_2Si_5N_8$ powders are in good agreement with the reported powder patterns in JCPDS 82–2489, 85–101 and 85–102, respectively.

2.4. Optical measurements

The diffuse reflectance, emission and excitation spectra of the samples were measured at room temperature by a Perkin Elmer LS 50B spectrophotometer equipped with a Xe flash lamp. The reflection spectra were calibrated with the reflection of black felt (reflection 3%) and white barium sulfate ($BaSO_4$, reflection ~100%) in the wavelength region of 230–700 nm. The excitation and emission slits were set at 15 nm. The emission spectra were corrected by dividing the measured emission intensity by the ratio of the observed spectrum of a calibrated W-lamp and its known spectrum from 300 to 900 nm. Excitation spectra were automatically corrected for the variation in the lamp intensity (and thus for the spectral dependence of the excitation energy) by a second photomultiplier and a beam-splitter. All luminescence spectra were measured with a scan speed of 400 nm/min at room temperature in air.

3. Results and discussion

3.1. Diffuse reflection spectra of undoped and Mn^{2+}-doped $M_2Si_5N_8$ (M=Ca, Sr, Ba) samples

Figs. 1–3 show the diffuse reflection spectra of undoped and Mn^{2+}-doped $M_2Si_5N_8$ (M = Ca, Sr, Ba) samples. Both undoped and Mn^{2+}-doped samples show a remarkable drop in reflection in the UV range around 300 nm with an estimated band gap at about 250 nm for M = Ca, 265 nm for M = Sr and 270 nm for M = Ba. This also have been observed in the diffuse reflection spectra of Eu^{2+}-doped $M_2Si_5N_8$ (M = Ca, Sr, Ba) samples [4], corresponding to the valence-to-conduction band transitions of the $M_2Si_5N_8$

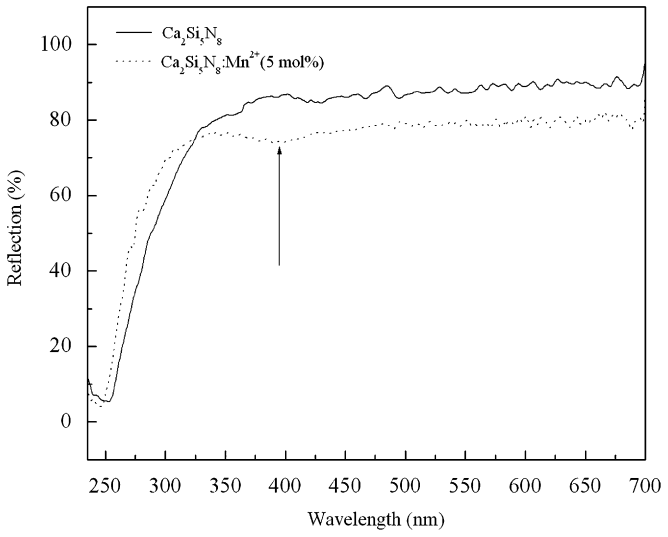

Fig. 1. Diffuse reflectance spectra of undoped and Mn^{2+}-doped $Ca_2Si_5N_8$ samples.

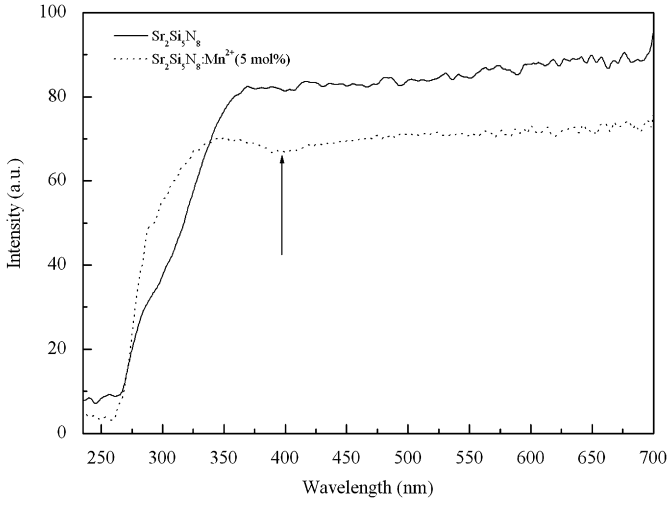

Fig. 2. Diffuse reflectance spectra of undoped and Mn^{2+}-doped $Sr_2Si_5N_8$ samples.

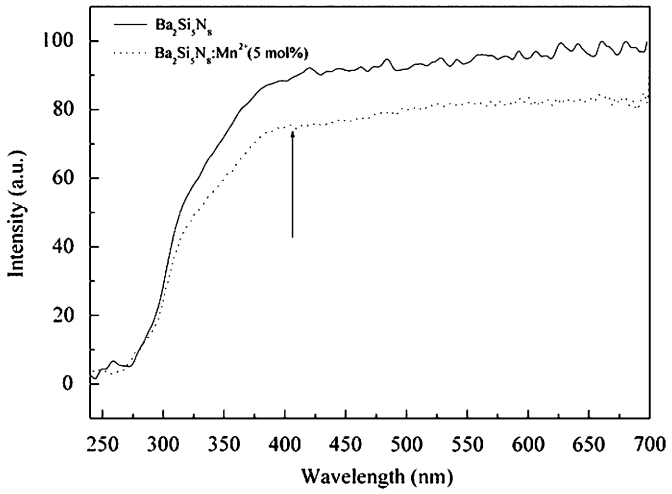

Fig. 3. Diffuse reflectance spectra of undoped and Mn^{2+}-doped $Ba_2Si_5N_8$ samples.

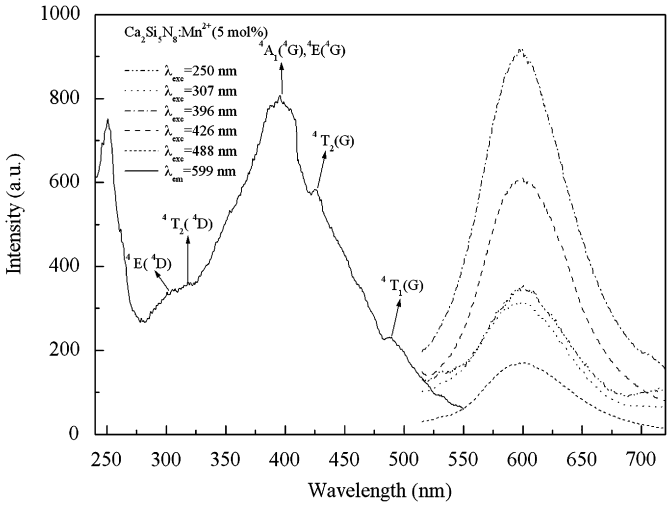

Fig. 4. Excitation and emission spectra of Mn^{2+}-activated $Ca_2Si_5N_8$ phosphor.

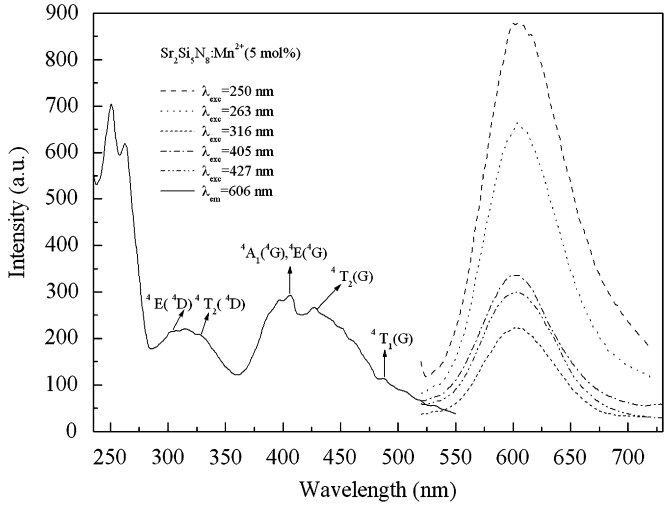

Fig. 5. Excitation and emission spectra of Mn^{2+}-activated $Sr_2Si_5N_8$ phosphor.

host lattice. The intense reflection in the visible spectral range is in agreement with the observed gray-white daylight color for undoped $M_2Si_5N_8$ samples. In the Mn^{2+}-doped samples, there is also present a weak absorption band in the wavelength range of 370–420 nm, which can be attributed to the transitions from the ground state $^6A_1(^6S)$ of Mn^{2+} to its excited states. Because the *d–d* transitions of Mn^{2+} are spin and parity forbidden, the absorption band of Mn^{2+} in the wavelength range of 370–420 nm in the host lattice of $M_2Si_5N_8$ (M = Ca, Sr, Ba) is only weak, which is in good agreement with the observed gray-white daylight color for Mn^{2+}-doped $M_2Si_5N_8$ samples.

3.2. Photoluminescence properties of Mn^{2+}-activated $M_2Si_5N_8$ (M = Ca, Sr, Ba) phosphors

Figs. 4–6 show the excitation and emission spectra of $M_2Si_5N_8:Mn^{2+}$ (M = Ca, Sr, Ba). All $M_2Si_5N_8:Mn^{2+}$ phosphors show narrow symmetric bands in the wavelength range of 500–700 nm with peak center at about 599, 606 and 567 nm for M = Ca, Sr, Ba, respectively, irrespective of the excitation wavelength (Figs. 4–6). The observed band emission is ascribed to the $^4T_1$ $(^4G)\rightarrow{}^6A_1(^6S)$ transition of Mn^{2+} in $M_2Si_5N_8$ host lattice. The excitation spectrum of $M_2Si_5N_8:Mn^{2+}$ (M = Ca, Sr, Ba) extends a broad range of wavelengths (230–500 nm) and is consistent with the diffuse reflectance spectra. Definitely, the short strong excitation bands below 300 nm originate from host lattice excitation as can be concluded from the comparison with the reflection spectrum. The appearance of the host lattice excitation bands in the excitation spectrum of Mn^{2+} indicates that there exists efficient energy transfer from the host lattice of $M_2Si_5N_8$ (M = Ca, Sr, Ba) to Mn^{2+} ions. The remaining excitation bands in the wavelength range of 300–500 nm can be assigned to the transitions of Mn^{2+} from ground state $^6A_1$ (^6S) to ^4E (^4D), $^4T_2$ (^4D), [$^4A_1(^4G)$,

$^4E(^4G)$], $^4T_2$ (^4G) and $^4T_1$ (^4G) levels, respectively, as illustrated in Figs. 4–6. The energy level scheme and the main mechanisms involved in the generation of Mn^{2+} emission in $M_2Si_5N_8$ are shown in Fig. 7. The typical band emission of Mn^{2+} in $M_2Si_5N_8$ host lattice can be realized in two different ways. The first way is to excite the Mn^{2+} ion directly in its own excitation levels. The electron from the ground state of Mn^{2+} is excited into the higher energy levels of Mn^{2+}. The excited free electron then relaxes to the $^4T_1(^4G)$ excited state through $^4E(^4D)$, $^4T_2(^4D)$, ($^4A_1$, ^4E) (^4G) and $^4T_2(^4G)$ intermediate energy levels of Mn^{2+} by a non-radiative process, followed by a radiative transition from the $^4T_1(^4G)$ excited state to the $^6A_1(^6S)$ ground state giving rise the typical emission of Mn^{2+} in $M_2Si_5N_8$ host lattice. The second option is to excite host lattice, followed by efficient energy transfer from the host lattice to the Mn^{2+} ion, which also results in the typical emission of Mn^{2+}.

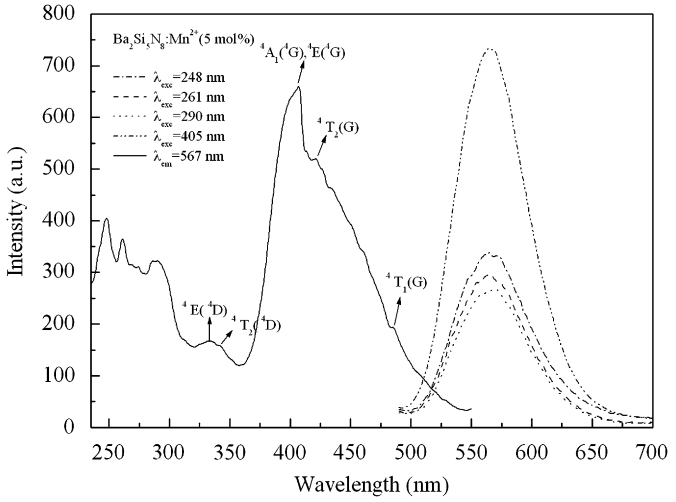

Fig. 6. Excitation and emission spectra of Mn^{2+}-activated $Ba_2Si_5N_8$ phosphor.

Table 1 summarizes the characteristics of $M_2Si_5N_8$:Mn^{2+} (M = Ca, Sr, Ba) phosphors and compares them with some other typical Mn^{2+}-doped phosphors. The luminescence properties of Mn^{2+}-doped $M_2Si_5N_8$ (M = Ca, Sr, Ba) are influenced by the crystal structure of host lattice ($Ca_2Si_5N_8$ versus $Sr_2Si_5N_8$ and $Ba_2Si_5N_8$) and the size of the M ion ($Sr_2Si_5N_8$ versus $Ba_2Si_5N_8$) (Table 1). For the isostructural compounds of $Sr_2Si_5N_8$ and $Ba_2Si_5N_8$, the metal-ligand distances are smaller in $Sr_2Si_5N_8$ than in $Ba_2Si_5N_8$ [Sr_1–N = 2.865(6) Å versus Ba_1–N = 2.917(3) Å, Sr_2–N = 2.928(7) Å versus Ba_2–N = 2.981(5) Å] because Ba^{2+} is larger than Sr^{2+} [26]. As a consequence, the crystal field strength is larger for Mn^{2+} in $Sr_2Si_5N_8$ than in $Ba_2Si_5N_8$ host lattice, which results in the longer (about 30 nm) wavelength emission band of Mn^{2+} in $Sr_2Si_5N_8$ than in $Ba_2Si_5N_8$ host lattice. Because Ca^{2+} is smaller than Sr^{2+}/Ba^{2+}, an even longer emission wavelength would be expected for Mn^{2+} in $CaSi_5N_8$ host lattice. However, this is not the case, evidently as a consequence of $Ca_2Si_5N_8$ having a different crystal structure and a different coordination environment for (and thus crystal field around) the Ca ion as compared with $M_2Si_5N_8$ (M = Sr, Ba) [27,28].

In addition, there is present only a single narrow emission band in the luminescence spectra of Mn^{2+}-doped $M_2Si_5N_8$ phosphors although there are present two different crystallographic M sites in $M_2Si_5N_8$ (M = Ca, Sr, Ba) [1,6,27,28] on which Mn^{2+} potentially can substitute. The trivial reason of absence of two Mn^{2+} emission bands because of similar environment for Mn^{2+}

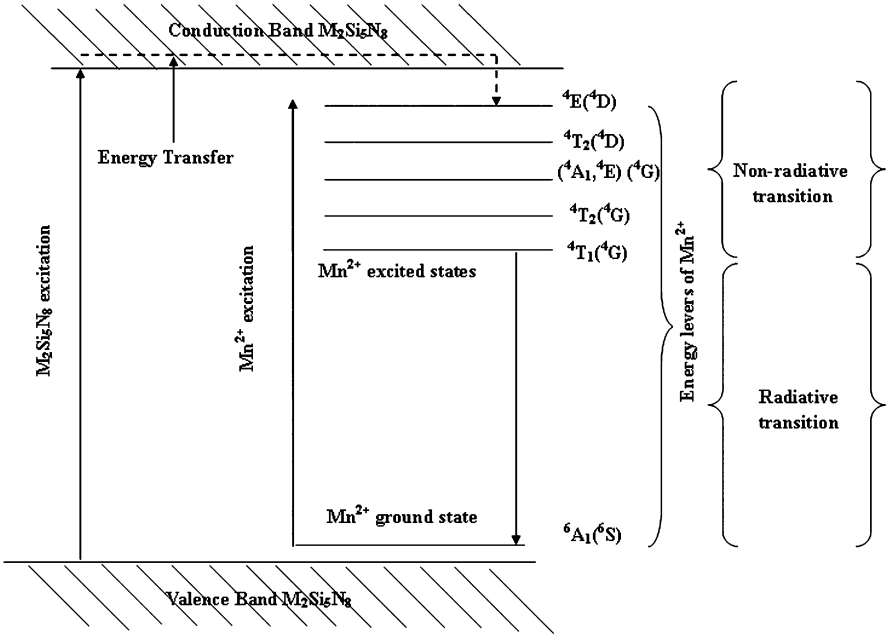

Fig. 7. Energy level scheme of $M_2Si_5N_8$:Mn^{2+} phosphor.

Table 1
Characteristics of Mn^{2+}-doped $M_2Si_5N_8$ (M = Ca, Sr, Ba) phosphors as compared to those of typical Mn^{2+}-doped phosphors at room temperature

Phosphors	$Ca_2Si_5N_8$:Mn^{2+}	$Sr_2Si_5N_8$:Mn^{2+}	$Ba_2Si_5N_8$:Mn^{2+}	$ZnSiN_2$:Mn^{2+}	Zn_2SiO_4:Mn^{2+}	Ba_2ZnS_3:Mn^{2+}
Crystal system	*Cc*	*Pmm*2_1	*Pmm*2_1	*Pna*2_1	*RH*	*Pnam*
Body color	Grey-white	Grey-white	Grey-white	Grey-white	Grey-white	Grey-white
Host absorption edge (nm)	250	265	270	250	175, 250	360
Absorption bands of Mn^{2+} (nm)	370–420	370–420	370–420			
Excitation bands (nm)	250, 307, 396, 426, 489	250, 263, 316, 405, 427, 488	248, 261, 290,436 405, 421, 486	260, 390, 420, 470, 490	175, 251	350, 410, 510
Emission maximum (nm)	599	606	567	620	520	625
Full width at half maximum broadband (nm)	70	60	60		40	60–70
Reference	This work	This work	This work	[24]	[10,30]	[20–22]

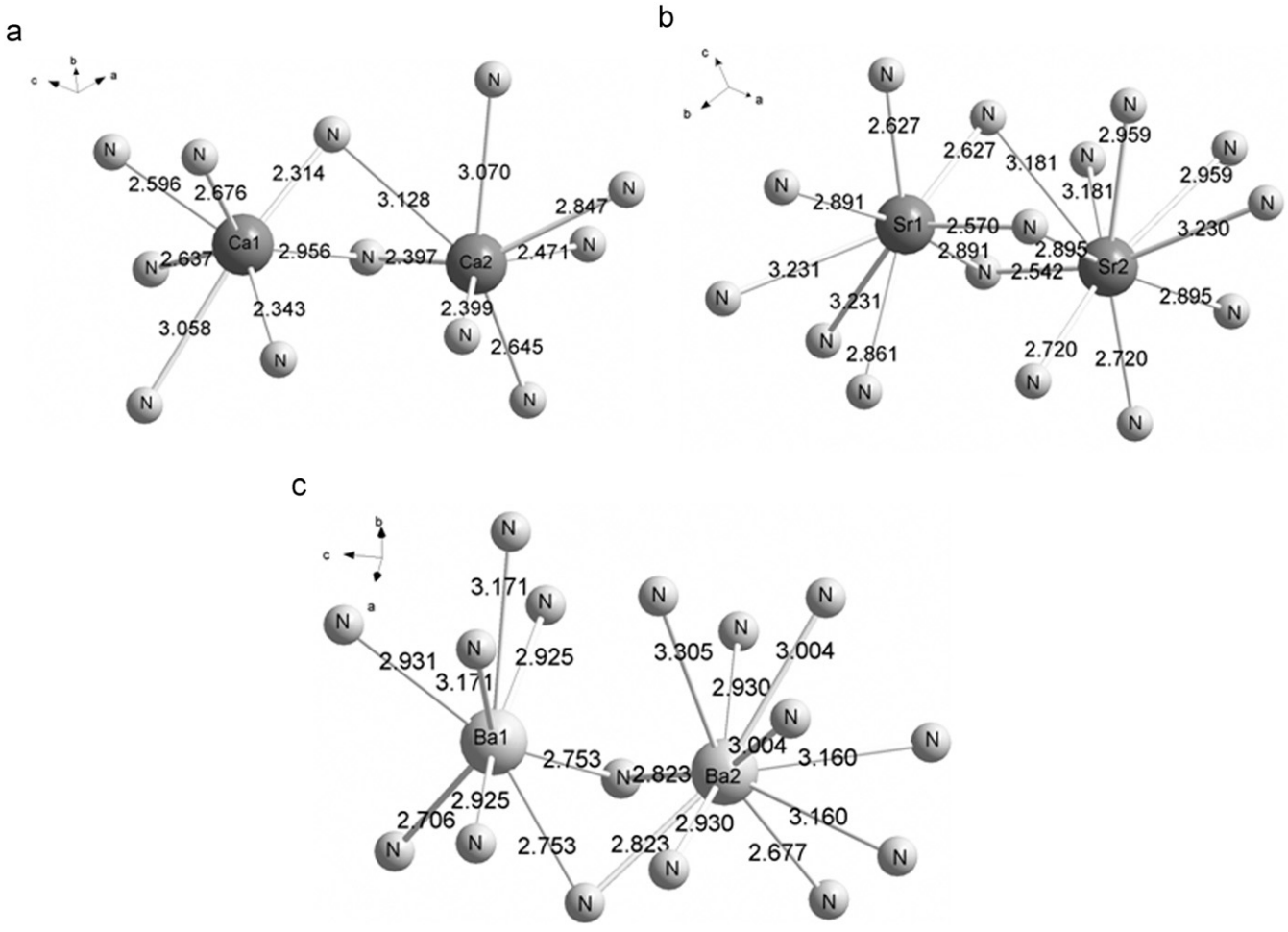

Fig. 8. Coordination environment of the M atoms and the M–N distances (Å) in $M_2Si_5N_8$: (a) M = Ca, (b) M = Sr and (c) M = Ba.

in two different sites, which eventually results in large overlap of the two emission bands of Mn^{2+} in $M_2Si_5N_8$, can be ruled out because crystal structure data show that the environment of the two M sites is very different in $M_2Si_5N_8$ (M = Ca, Sr, Ba). For the isostructural compounds $M_2Si_5N_8$ (M = Sr, Ba), the coordination numbers are 8 and 10 for M_1 and M_2 sites, respectively, while the coordination numbers are both 7 for Ca_1 and Ca_2 sites in $Ca_2Si_5N_8$ host lattice (Fig. 8). In addition, the mean distance M_1–N is smaller than that of M_2–N in all $M_2Si_5N_8$ (M = Ca, Sr, Ba) compounds [Ca_1–N = 2.653(7) Å versus Ca_2–N = 2.708(7) Å, Sr_1–N = 2.865(6) Å versus Sr_2–N = 2.928(7) Å, Ba_1–N = 2.917(3) Å versus Ba_2–N = 2.981 (5) Å] (Fig. 8). Thus it is evident that there would be a large difference in coordination environment (and thus crystal field) for Mn^{2+} in two different M sites, especially

in $M_2Si_5N_8$ (M = Sr, Ba) host lattice. Another possibility is that the luminescence properties of Mn^{2+} are not sensitive to the change of the local structure. However, this option can also be ruled out because of the observed difference in the luminescence properties of Mn^{2+} for the $M_2Si_5N_8$ depending on M type (Table 1). Therefore, probably only one M site is occupied by Mn^{2+} due to the large size difference between it and the M^{2+} ions ($r_{Mn}^{2+} \ll r_M^{2+}$). This is consistent with the fact that varying the excitation wavelength yields similar emission spectra (Figs. 4–6). As indicated above, the mean distance M_1–N is smaller than that of M_2–N. As a consequence, the dopant Mn^{2+} ions may prefer to substitute the smaller M_1 site in the $M_2Si_5N_8$ (M = Ca, Sr, Ba) host lattice because of best matching of ionic sizes. The exact explanation is subject of further study. The half-width for the single narrow emission band of $M_2Si_5N_8$:Mn^{2+} phosphors is about 60 nm for M = Sr and Ba, and 70 nm for M = Ca, which resembles with the literature values, e.g. about 70 nm for $Zn_3(PO_4)_2$:Mn^{2+} [29], 60 nm for Ba_2ZnS_3:Mn^{2+} [20–22] and 40 nm for Zn_2SiO_4:Mn^{2+} [30]. This half-width is significantly smaller than that of red Eu^{2+} emission (~100 nm) in $M_2Si_5N_8$ host lattices [4].

The $3d^5$ multiplet energies of Mn^{2+} in host lattices depend largely on the crystal field and the covalent interaction with the host lattice because the 3d electrons of the transition metal ions are outermost electrons. It is well known that Tanabe–Sugano diagrams explain very well the characteristics of optical spectra due to the intra-3d shell transition of transition metal ions in host lattices. According to the diagram for the $3d^5$ electron configuration of Mn^{2+} [31–33], the energies of the $^4E(^4G)$, $^4A_1(^4G)$ states and $^4E(^4D)$ state relative to the $^6A_1(^6S)$ ground state are insensitive to the crystal-field strength Dq and is determined only by the Racah parameter B. The B value depends largely on the covalent interaction between Mn^{2+} and surrounding ligand and decreases from the free-ion value with increase of the covalent interaction (the nephelauxetic effect [34]). On the other hand, the Tanabe–Sugano diagram predicts that the energy separations between the $^4T_1(^4G)$ and $^4T_2(^4G)$ states and the $^6A_1(^6S)$ ground state are very sensitive to the crystal-field strength Dq and decreases with increase of crystal field strength. It is well known that the emission bands of Mn^{2+} originate from the $^4T_1(^4G) \rightarrow {}^6A_1(^6S)$ transition. Therefore, the position of the emission bands of Mn^{2+}-doped phosphors is largely determined by the crystal filed strength of Mn^{2+} in the host lattice. As a consequence, the wavelength position of the emission band of Mn^{2+} depends strongly on the host lattice. For Mn^{2+}-doped phosphors in general, the emission bands can vary from the green to the deep red region of the electromagnetic spectrum [23]. Mn^{2+} usually gives a green emission when it is located on a lattice site with weak crystal-field, whereas it gives an orange to deep red emission on a strong crystal-field site. Due to the large crystal-field effect induced by the coordinating nitrogen ion, Mn^{2+} shows an orange to red emission in $M_2Si_5N_8$ (M = Ca, Sr, Ba) and even a deep red emission in $MSiN_2$ (M = Zn, Mg, Ca) host lattice (Table 1) [24,25]. As a conclusion, the long-wavelength emission of Mn^{2+} in $M_2Si_5N_8$ host lattice can be attributed to the effect of a strong crystal-field of Mn^{2+} in nitrogen coordination environment.

The absorption and excitation bands of $M_2Si_5N_8$:Mn^{2+} perfectly match with the radiation of the UV-emitting InGaN based LEDs in the range of 370–420 nm, so in combination with other phosphors these materials are capable of generating white light. However, due to the forbidden d–d transitions of Mn^{2+}, Mn^{2+}-doped $M_2Si_5N_8$ only show weak absorption in the range of 370–420 nm, so for white LED lighting applications this absorption has to be increased by use of suitable sensitizer ions. It is interesting to note that the Mn^{2+}-activated $M_2Si_5N_8$ (M = Ca, Sr, Ba) phosphors not only show strong absorption at 254 nm because of the host lattice absorption, but also that the host lattices can efficiently transfer the absorbed energy to Mn^{2+} ions resulting in the typical yellow or red emissions of Mn^{2+} ions, making them also interesting for potential applications in the field of low-pressure mercury discharge lamps.

4. Conclusions

Mn^{2+}-activated $M_2Si_5N_8$ (M = Ca, Sr, Ba) phosphors have been prepared by a solid-state reaction successfully and their photoluminescence properties were investigated. As compared to red Eu^{2+} emission in these host-lattices, the Mn^{2+}-activated $M_2Si_5N_8$ phosphors exhibit narrow emission bands with maxima at about 599, 606 and 567 nm for M = Ca, Sr, Ba, respectively. $M_2Si_5N_8$:Mn^{2+} samples are attractive LED phosphors with respect to the position of the absorption (370–420 nm) and emission (500–700 nm) bands. However, the absorption strength of $M_2Si_5N_8$:Mn^{2+} phosphors in the wavelength range of 370–420 nm has to be enhanced to increase their potential for white LED lighting applications. In addition, it is worth noting that $M_2Si_5N_8$:Mn^{2+} phosphors may be of interest for applications in the field of low-pressure mercury discharge lamps.

Acknowledgments

The authors gratefully acknowledge financial support from Leuchtstoffwerk Breitungen GmbH Company (Germany). The authors also wish to thank M.M.R.M. Hendrix for his support with XRD measurements, H.A.M. van der Palen for maintenance of the furnaces, and Dr. Detlef Starick and Dr. Sylke Rösler for helpful discussions.

References

[1] H.A. Höppe, H. Lutz, P. Morys, W. Schnick, A. Seilmeier, J. Phys. Chem. Solids 61 (2000) 2001.

[2] J.W.H. van Krevel, Ph.D. Thesis, Eindhoven University of Technology, 2000.
[3] Y.Q. Li, Ph.D. Thesis, Eindhoven University of Technology, 2005.
[4] Y.Q. Li, J.E.J. van Steen, J.W.H. van Krevel, G. Botty, A.C.A. Delsing, F.J. DiSalvo, G. de With, H.T. .Hintzen, J. Alloys Compd. 417 (2006) 273.
[5] R.J. Xie, N. Hirosaki, T. Suehiro, F.F. Xu, M Mitomo, Chem. Mater. 18 (2006) 5578.
[6] X.Q. Piao, T. Horikawa, H. Hanzawa, K. Machida, Appl. Phys. Lett. 88 (2006) 161908.
[7] Y.Q. Li, G. de With, H.T. Hintzen, J. Lumin. 116 (2006) 107.
[8] X.Q. Piao, T. Horikawa, H. Hanzawa, K. Machida, J. Electrochem. Soc. 153 (12) (2006) H232.
[9] R. Mueller-Mach, G. Mueller, M.R. Krames, H.A. Hoeppe, F. Stadler, W. Schnick, T. Juestel, P. Schmidt, Phys. Stat. Sol. (a) 202 (2005) 1727.
[10] R.P. Sreekanth Chakradhar, B.M. Nagabhushana, K.P. Ramesh, J.L. Rao, J. Chem. Phys. 121 (2004) 10250.
[11] D.Y. Lee, Y.C. Kang, H.D. Park, S.K. Ryu, J. Alloys Compd. 353 (2003) 252.
[12] Y. Hattori, T. Isobe, H. Takahashi, S. Itoh, J. Lumin. 113 (1,2) (2005) 69.
[13] Y. Takahashi, T. Isobe, Jpn. J. Appl. Phys. Part 1 442 (2) (2005) 922.
[14] A.L. Smith, J. Electrochem. Soc. 98 (1951) 363.
[15] J.K. Berkowitz, J.A. Olsen, J. Lumin. 50 (1991) 111.
[16] J.S. Kim, P.E. Jeon, J.C. Choi, H.L. Park, Appl. Phys. Lett. 84 (2004) 2931.
[17] W.J. Yang, L.Y. Luo, T.M. Chen, N.S. Wang, Chem. Mater. 17 (2005) 3883.
[18] W.J. Yang, T.M. Chen, Appl. Phys. Lett. 88 (2006) 101903.
[19] Y.H. Won, H.S. Jang, W.B. Im, D.Y. Jeon, Appl. Phys. Lett. 89 (20006) 231909.
[20] X.M. Zhang, H.P. Zeng, Q. Su, J. Allloys Compd. 441 (2007) 259.
[21] Y.F. Lin, Y.H. Chang, Y.S. Chang, B.S. Tsai, Y.C. Li, J. Alloys Compd. 421 (2006) 268.
[22] P. Thiyagarajan, M. Kottaisamy, M.S. Ramachandra Rao, J. Phys. D: Appl. Phys. 39 (2006) 2701.
[23] G. Blasse, B.C. Grabmaier, Luminescent Materials, Springer, Berlin, 1994.
[24] K. Uheda, H. Takizawa, T. Endo, J. Mater. Sci. Lett. 20 (2001) 1753.
[25] V. Bonder, L. Axelrud, V. Davydov, T. Felter, Mater. Res. Soc. Symp. Proc. 639 (2001) G11.36.1.
[26] R.D. Shannon, Acta Crystallogr. A 32 (1976) 751.
[27] T. Schlieper, W. Milius, W. Schnick, Z. Anorg. Allg. Chem. 621 (1995) 1380.
[28] T. Schlieper, W. Schnick, Z. Anorg. Allg. Chem. 621 (1995) 1037.
[29] M. Saakes, M. Leskelä, G. Blasse, Mater. Res. Bull. 19 (1984) 83.
[30] V.B. Bhatkar, S.K. Omanwar, S.V. Moharil, Phys. Stat. Sol. (a) 191 (2002) 272.
[31] Y. Tanabe, S. Sugano, J. Phys. Soc. Jpn. 9 (1954) 753.
[32] Y. Tanabe, S. Sugano, J. Phys. Soc. Jpn. 9 (1954) 767.
[33] S. Sugano, Y. Tanabe, H. Kamimura, Multiplets of Transition-Metal Ions in Crystals, Academic Press, New York, 1970.
[34] J.S. Griffith, The Theory of Transition-Metal Ions, Cambridge University Press, Cambridge, 1961.